Journal of Nuclear Materials 383 (2008) 172–177

Contents lists available at ScienceDirect

Journal of Nuclear Materials

journal homepage: www.elsevier.com/locate/jnucmat

Ageing of zirconium alloy components

S. Chatterjee *, Priti Kotak Shah, J.S. Dubey

Post Irradiation Examination Division, Bhabha Atomic Research Centre, Mumbai 400 085, India

ARTICLE INFO

PACS:
81.40.Wx
28.41.Qb

ABSTRACT

India has two types (pressurized heavy water reactors (PHWRs) and boiling water reactors (BWRs)) of commercial nuclear reactors in operation, in addition to research reactors. Many of the life limiting critical components in these reactors are fabricated from zirconium alloys. The progressive degradation of these components caused by the cumulative exposure of high energy neutron irradiation with increasing period of reactor operation was monitored to assess the degree of ageing. The components/specimens examined included fuel element claddings removed from BWRs, pressure tubes and garter springs removed from PHWRs and calandria tube specimens used in PHWRs. The tests included tension test (for cladding, garter spring), fracture toughness test (for pressure tube), crush test (for garter spring), and measurement of irradiation induced growth (for calandria tube). Results of various tests conducted are presented and applications of the test results are elaborated for residual life estimation/life extension of the components.

1. Introduction

Pressurized heavy water reactors (PHWRs) have multiple numbers of horizontally mounted coolant channels within a horizontally supported stainless steel cylindrical vessel called calandria. Each coolant channel assembly comprises of a pressure tube (PT), a calandria tube (CT) and garter springs (GS) that are made from zirconium alloys. Natural uranium oxide, in the form of pellets and encapsulated in thin Zircaloy cladding, forms the fuel pins of the PHWRs. Several such pins are assembled in the form of fuel bundles and are loaded in the pressure tubes. Inside PTs heavy water coolant flows at a pressure of ~10 MPa and at a temperature of ~300 °C. Calandria tubes surround the pressure tubes from outside. Annulus spacers (garter springs) are provided at regular intervals in the annular space to support pressure tube and to prevent it from contacting the calandria tube. CTs are surrounded by low pressure, low temperature heavy water moderator maintained at 60 °C in the calandria vessel. Enriched uranium-dioxide pellets encapsulated in Zircaloy claddings form the fuel elements of the boiling water reactors (BWRs). Several such assembled elements that form fuel bundles are exposed inside the reactor to coolant pressure of ~7 MPa and temperature of ~300 °C.

These zirconium alloy components are located in the core region of the reactor and thus are exposed to high energy neutron of very high intensity. Neutron irradiation is the most important source of damage in zirconium alloys. The damage is manifested in one or more form of (a) dimensional changes, (b) increase in tensile strength and reduction in ductility, (c) increase in transition temperature, (d) decrease in fracture toughness, (e) increase in crack growth rates and (f) changes in microstructure/chemical composition. One or some of these changes may limit life of these components. Information on in-service behaviour and extent of ageing induced degradation of the zirconium alloy components are, therefore, justifiably useful for uninterrupted safe running of nuclear power plants.

This paper presents the evaluation carried out over the years of tensile properties of Zircaloy-2 claddings from reactor operated fuel pins, fracture properties of Zircaloy-2 pressure tubes, irradiation enhanced deformation of Zr–2.5Nb pressure tube, and behaviour of Zr–2.5Nb–0.5Cu garter springs removed from Indian PHWRs, and irradiation induced growth of seamless Zircaloy calandria tubes, used in Indian PHWRs.

2. Experimental approach

2.1. Tensile properties of Ziracloy claddings

Ring specimens of 5 mm width cut from Zircaloy cladding of reactor operated fuel elements that had experienced 5000–15 000 MW d/t of fuel burnup were subjected to ring tensile testing. To minimize the bending stresses and to restrict the initial portion of the elongation not confined within the specimen gage length, special care was taken to match the contour of the two half pieces of the mandrel constituting the grip with the contour of the specimen rings. The true stress–true strain data points up to the onset of the necking from the individual load elongation curves of the specimens were used as input data in Voce's equation. The

* Corresponding author. Tel.: +91 22 2559 4927; fax: +91 22 2550 5151.
E-mail address: schat@barc.gov.in (S. Chatterjee).

0022-3115/$ - see front matter © 2008 Elsevier B.V. All rights reserved.
doi:10.1016/j.jnucmat.2008.08.039

semi-empirical approach of treating the data points with Voce's equation resulted in minimization of the uncertainty in uniform elongation data caused by the uncertainty inherently associated with the ring tensile test method [1].

2.2. Fracture properties of Zircaloy-2 pressure tubes

Transverse tension (ring) specimens with 25 mm gauge length and 5 mm width were fabricated inside hot cells from 12.5 mm wide ring sections cut from suitable locations, corresponding to coolant outlet end (highest hydrogen equivalent content and irradiation temperature), and coolant inlet end (lowest irradiation temperature) and at mid-length (highest neutron fluence exposure). Tension tests were carried out on these specimens in the temperature range of 200–300 °C using a remotized screw driven universal testing machine. The tensile properties were utilized to compute the fracture toughness and the critical crack length (CCL) of the pressure tubes.

The CCL ($2a$) for the pressure tube was estimated [2] by finding the value of the semi-crack length (a) which satisfied the following equation at the hoop stress (S_H) corresponding to the reactor operating pressure:

$$J_{max} = \left(\frac{8aS_f^2}{\pi E}\right) \ln\left[\sec\left(\frac{\pi M S_H}{2S_f}\right)\right] \quad (1)$$

S_f and M being the flow stress and Folia's factor, respectively. The values of J_{max} were obtained from the transverse tensile properties obtained from ring tension tests as per the relation:

$$J_{max} = 2.8\beta_{Zr}^2 S_y \varepsilon_f n^2 \quad (2)$$

where S_y is the yield strength, n is strain hardening exponent and ε_f is fracture ductility, and E is elastic modulus. The value of n is from the equation $S = K\varepsilon^n$. The appropriate values of β_{Zr} were obtained experimentally and were found to depend on the test temperature [3].

The pressure tubes evaluated had experienced up to 9.5 effective full power years (EFPYs) of operation and had hydrogen equivalent contents up to 200 ppm. The inventory of the pressure tube sections evaluated is given in Table 1.

2.3. Mechanical properties of garter springs

Garter springs, fabricated out of rectangular wires of Zr–2.5% Nb–0.5% Cu alloy by coiling and having a girdle wire running inside, were subjected to detailed mechanical property evaluation by carrying out stretch test, tension test and crush test. The girdle wire was first removed from the GS assembly so that the subsequent mechanical tests could be carried out on the spring portion alone.

Integrity of each link in the entire spring was ascertained by subjecting the entire portion of the spring to applied load up to 9 kg in steps. Subsequently tension test on small pieces of GS from the 6 O'clock location were conducted. Some more number of small pieces were subjected to crush test.

Crush tests, that simulated the loading of GS under in-reactor condition, were carried out using small pieces from the region around 6 O'clock as well as 3 O'clock location. The test was accomplished with the help of a special fixture, which consisted of a pair of semi-circular mandrels surrounded by a rigid ring. The dimension of the mandrels corresponded to the outer diameter of the pressure tube. The inner diameter of the rigid ring was that of the calandria tube. The GS piece to be subjected to crush test was kept in the space between the mandrels and the ring, and the loading was progressively increased until the piece got crushed or the gap between the mandrel and the rigid ring got closed. Further details are available elsewhere [4]. The inventory of the garter springs evaluated is given in Table 2.

2.4. Creep and growth in Zr–2.5Nb pressure tube

The diametral changes at discrete locations along the length of a pressure tube S-07 from Kakrapar Atomic Power Station-2 (KAPS-2), which had undergone 8 EFPYs of reactor operation, were measured. The corresponding flux (ϕ) and temperature (T) at these locations along the length of the pressure tube, were calculated using appropriate codes. Texture, grain structure, dislocation density and chemistry (oxygen) were assumed to be constant along the length of PT. The calculation of diametral change (ΔD) is based on deformation model developed in-house that considered three mechanisms [5] (irradiation creep, irradiation growth and thermal creep) as reported in open literature. Contribution by thermal creep was included in the irradiation creep component. The contributions by irradiation creep and irradiation growth has been assumed to be additive. The following empirical equation was used.

$$\Delta D = \Delta\check{D} \cdot t = \left[A \times \sigma \times \phi \times \exp\left(\frac{-Q_c}{RT}\right)\right] + \left[B \times \phi \times \exp\left(\frac{-Q_g}{RT}\right)\right] \cdot t \quad (3)$$

where Q_c is the activation energy for creep, Q_g is the activation energy for growth, $\Delta\check{D}$ is the rate of change in pressure tube diameter, σ *is the* average of hoop stress experienced by the pressure tube at inlet and outlet ends, ϕ is the fast neutron flux ($E > 1$ MeV), T is the temperature in K, t *is the* time of in-reactor residence and R is universal gas constant.

The parameters A, B, Q_c and Q_g were calculated by substituting the respective values of ΔD, ϕ, σ, T and t for each discrete locations and iterating the sets of equations so obtained.

2.5. Irradiation growth in calandria tubes

Irradiation growth specimens (100 mm long, 12 mm wide and 1.5 mm thick) fabricated from seamless and seam welded calandria tube pieces manufactured at Nuclear Fuel Complex, Hyderabad were sectioned with their direction of measurement parallel to the axis of tube (longitudinal specimens) and those with their

Table 1
Inventory of pressure tubes evaluated

Reactor	EFPY	H_{eq} (ppm)	Location
MAPS-2	4.8	39	N-10, outlet end
MAPS-1	6.25	22	P-13, mid-length
MAPS-1	6.25	22	P-13, inlet end
RAPS-2	8.25	84	K-7, outlet end
RAPS-2	8.25	40	K-7, mid-length
MAPS-1	9.5	200	J-7, outlet end
MAPS-1	9.5	200	J-7, inlet end
MAPS-1	9.5	70	J-7, mid-length

Table 2
Inventory of garter springs evaluated

Spring identification	Reactor	EFPY	Numbers of specimens examined (type of test)
K-7	RAPS-2	8.25	1 (tension, stretch and crush tests)
O-11	RAPS-2	6.5	1 (tension, stretch and crush tests)
F-10	RAPS-1	3.6	2 (stretch test)
N-10	MAPS-2	4.8	1 (stretch and crush tests)
K-14	MAPS-2	3.6	1 (stretch and crush tests)
K-19	NAPS-1	1.8	1 (stretch and crush tests)
–	RAPS-2	8.25	14 (stretch test)

long axis perpendicular to this direction (transverse specimens). Transverse specimens were cold flattened, machined and annealed under vacuum. The specimens were loaded in aluminum tiers for irradiation in the reactor and one specimen was kept for reference in the hot cell. The initial measurement of each specimen was carried out by LVDT on the growth measuring jig prior to its loading in the aluminum tiers. For the measurement of fast neutron flux ($E > 1$ MeV) during irradiation four fast neutron flux monitors (Ni, Fe, Cu and Ti) encapsulated in a cadmium container, were loaded in each of the tiers. The detailed metallographic examination and basal pole texture coefficient evaluation of the seam welded and seamless calandria tube specimens were carried out. Mechanical properties of the seamless calandria tubes were also evaluated.

Irradiation was carried out at 80 °C in Dhruva research reactor up to an estimated fluence of 1×10^{25} n/m^2 ($E > 1$ MeV). The growth measurement was carried out on the specimens loaded in the tier (without removing the tier). The difference between the length before and after irradiation indicated irradiation induced growth of the specimens.

2.6. Delayed hydride cracking in Zircaloy-2 pressure tubes

The conditions that lead to delayed hydride cracking (DHC) were simulated by loading hydrided and fatigue precracked curved compact tension (CCT) specimens fabricated from Zircaloy-2 PTs and subjecting them to temperature–stress cycle. The loads corresponded to a stress intensity factor exceeding 16 MPa m$^{0.5}$. The specimens contained 115, 123 and 217 ppm of hydrogen. Tests were carried out at 290 and 250 °C using ΔT (soaking temperature – test temperature) up to 80 °C. Heating to the peak temperature was at the rate of 5 °C/min and cooling to the test temperature was at the rate of 1 °C/min. Incubation period and DHC growth rate was monitored using DCPD system. Details of the experimental setup and test procedures are published elsewhere [6].

3. Results

3.1. Tensile properties of Ziracloy claddings

Fig. 1 depicts the values of tensile strength and uniform elongation of the claddings evaluated. The ultimate tensile strength of the irradiated claddings shows increase of about 25% over the unirradiated value. The corresponding values of uniform elongation decrease up to 3.1% from the unirradiated value of 12.3%.

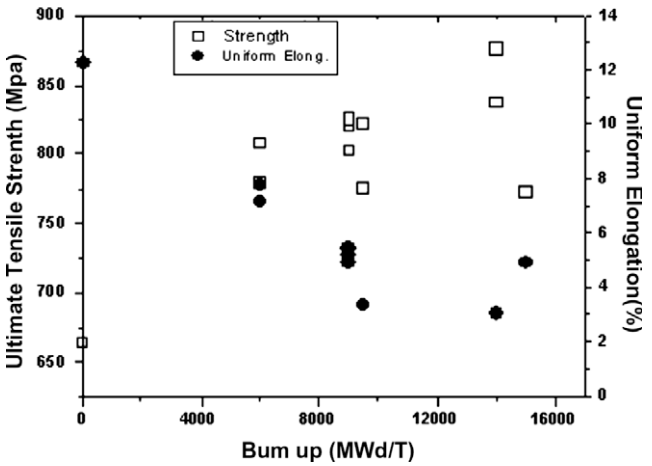

Fig. 1. Ambient temperature tensile properties of irradiated Zircaloy-2 claddings.

3.2. Fracture properties of Zircaloy-2 pressure tubes

Fig. 2 shows the CCL evaluated for the four Zircaloy-2 pressure tubes from the respective values of fracture toughness estimated at temperatures 200, 250 and 300 °C. These PTs had experienced reactor operation in excess of 4.0 EFPY. Therefore the respective values of CCL have been plotted with respect to the respective H_{eq} content. The CCL at the inlet end was calculated at hoop stress of 100 MPa (corresponding to the coolant pressure at the inlet end) and at the corresponding coolant temperature of 250 °C. Similarly at the outlet end was calculated at the corresponding hoop stress of 90 MPa and at temperature of 300 °C. The values of CCL of all the PTs evaluated, except PT J-07 were in excess of 60 mm.

3.3. Mechanical properties of garter springs

Tension tests conducted on representative pieces from two GSs, O-11 and K-07 (experienced EFPY of 6.5 and 8.25, respectively) showed that the former could withstand a tensile load of 196 N and later a load of 209 N. These results indicated the possibility of saturation in tensile properties beyond 6.5 EFPY. The results of crush tests carried out on GSs are given in Table 3. Only one GS piece out of two pieces belonging to 6 O'clock location of K-07 got crushed at a load of ~720 N/coil.

3.4. Creep and growth in Zr–2.5Nb pressure tube

Fig. 3 shows the estimated creep and growth components resulting from irradiation enhanced creep and irradiation induced growth in a Zr–2.5Nb PT that had experienced 8.0 EFPY of operation in KAPS-2 PHWR. The measured diametral changes are plotted

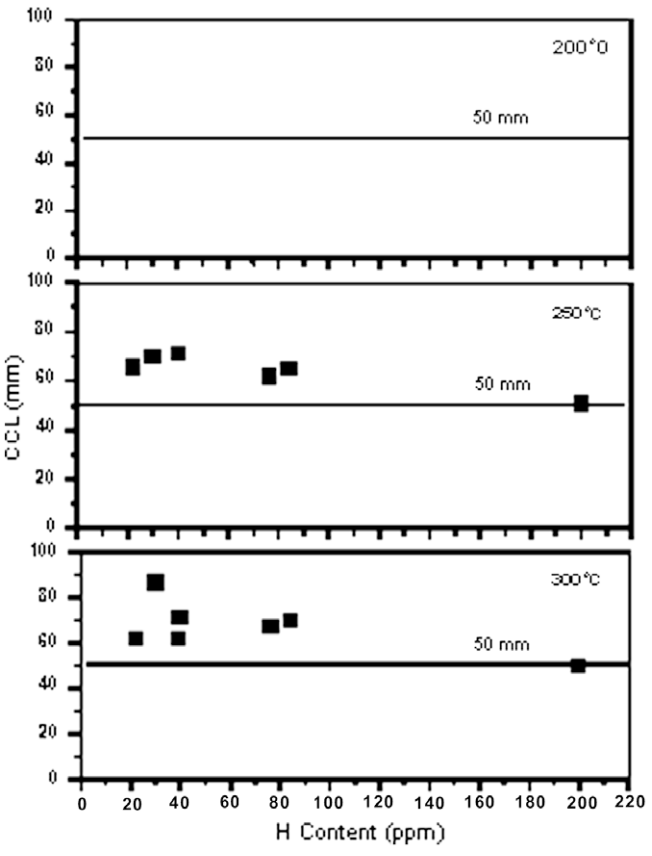

Fig. 2. Critical crack length for irradiated Zircaloy-2 pressure tubes.

Table 3
Room temperature crush test results for garter springs

Sl. no.	Spring identification (reactor, EPFY)	Location of GS piece	Maximum load applied (N/coil)	Remarks*
1	K-7(RAPS-2, 8.25)	6 O'clock	728	a
2	K-7(RAPS-2, 8.25)	6 O'clock	1078	b
3	K-7(RAPS-2, 8.25)	3 O'clock	667	b
4	K-7(RAPS-2, 8.25)	3 O'clock	556	b
5	O-11(RAPS-2, 6.5)	6 O'clock	845	b
6	O-11(RAPS-2, 6.5)	6 O'clock	716	b
7	N-10(MAPS-2, 4.8)	6 O'clock	539	b
8	N-10(MAPS-2, 4.8)	6 O'clock	440	b
9	N-10(MAPS-2, 4.8)	6 O'clock	405	b
10	K-14(MAPS-2, 3.6)	6 O'clock	410	b
11	K-14(MAPS-2, 3.6)	6 O'clock	474	b
12	K-14(MAPS-2, 3.6)	6 O'clock	563	b
13	K-19(NAPS-1, 1.8)	6 O'clock	428	b
14	K-19(NAPS-1, 1.8)	6 O'clock	425	b

* a; Specimen got crushed and b; gap got closed.

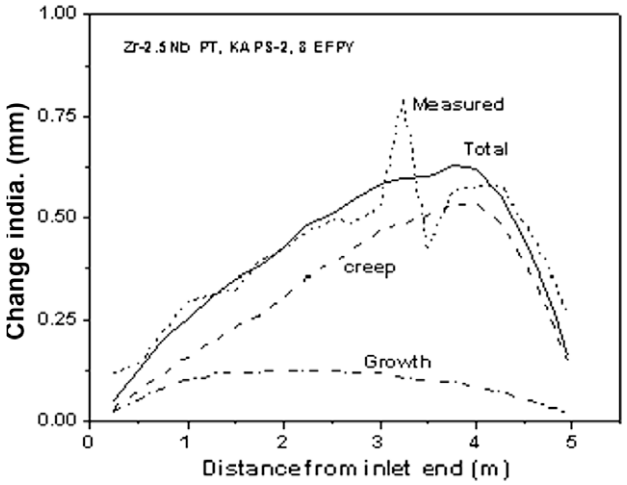

Fig. 3. Measured and calculated change in diameter of a Zr–2.5Nb pressure tube.

in the figure. The increase in inner diameter was predicted to be 0.76% over the unirradiated value of 82.5 mm.

3.5. Delayed hydride cracking in Zircaloy-2 pressure tubes

The results obtained from DHC tests are given in Table 4. The DHC velocity at 290 °C was found to be higher than 250 °C due to higher hydrogen diffusivity. It may be noted that even for specimen containing 115 ppmw of H, which is significantly higher than the terminal solid solubility limit for dissolution (TSSD) of hydrogen in zirconium matrix, the crack did not grow by DHC when ΔT used was 30 °C.

Table 4
Delayed hydride cracking test results for Zircaloy-2 pressure tubes

Sl. no.	H (ppm)	Test temperature (°C)	ΔT (°C)	DHC velocity (mm/h)	Average DHC velocity (mm/h)
1	115	290	80	0.113	0.116
2				0.120	
3			30	[a]	[a]
4		250	70	0.078	0.077
5				0.071	
6				0.083	
7	123			0.054	0.078
8				0.073	
9				0.110	
10	217		50	0.050	0.05

[a] Crack did not grow over the test duration.

Table 5
Irradiation growth strain in the calandria tube specimens

Specimen	Average growth strain $\times 10^4$
Seamless longitudinal	4.70
Seam welded longitudinal	4.78
Seamless transverse	2.78
Seam welded transverse	3.89

3.6. Irradiation growth in calandria tubes

Table 5 gives the relative comparison of irradiation induced growth strain in specimens fabricated from seam welded and seamless calandria tubes. The respective growth strain in longitudinal specimens is within 2.0%.

4. Discussion

4.1. Fuel clad

During residence inside reactor uranium-dioxide fuel pellets attain higher temperature than cladding tubes and undergo swelling and cracking. The pellets come in contact with the cladding resulting in localized deformation (at regions in contact with open cracks in the pellets) of the cladding under multiaxial stresses. To minimize the clad rupture the clad should have adequate ductility (uniform elongation) and high strength.

The uniform elongations measured at ambient temperature are in the range of 3–8%. Published information [7,8] indicates that circumferential elongation values at 300 °C are not expected to be lower than that at ambient temperature. Possibility of lower ductility under multiaxial loading condition (such as in closed end burst test) in comparison to ductility as obtained in ring tension test has been reported [9]. However, the closed end burst test gives over-conservative value of ductility as the circumferential elongation is limited by the available uniform elongation together with the necking elongation from the first neck to form. On actual fuel pins multiple neckings occur. Further, the ring specimens evaluated being from operated fuel elements would already have strained due to their interaction with fuel during reactor operation. Therefore, uniform elongation values reported are in fact margins available after the fuel claddings were strained during

reactor operation. Thus the result would imply that reactor operated fuel claddings have enough ductility for attaining the design life.

4.2. Pressure tubes

Pressure tube is the final pressure boundary containment structure in PHWRs and safety demands that leak-before-break criterion is met with. This is achieved by assuring adequate fracture toughness of the pressure tubes during their stay in the reactor. Conservatively estimated, a crack of length six times the tube thickness becomes a detectable leaking crack. Fracture toughness level that ensures a critical crack length of 12 times the tube thickness (50 mm for Zircaloy-2 PTs) can be expected to satisfy leak-before-break criterion. The margin between critical crack length and leak length will take care of the adverse implication of crack growth by delayed hydride cracking, if any. Under normal operating condition of the reactors, the pressure tubes experience temperature ranging from 250 to 300 °C. In case of contact between pressure tube and calandria tube, the mean wall temperature of pressure tube may go down to 200 °C. There is a generic reduction in the fracture properties of the pressure tube at these temperatures due to the synergistic contribution of neutron irradiation and deuterium pick-up. The pressure tubes would be expected to have attained limiting reduction of fracture properties so far as contribution from irradiation is concerned (because the properties are expected to reach saturation value after 3–4 EFPYs).

Fig. 2 shows that all pressure tubes which had H_{eq} contents limited to 84 ppm (and had experienced 8.25 EFPY) had their values of CCL exceeding 60 mm, significantly higher than the threshold value of 50 mm. For the case of PT J-07, the critical crack length at the outlet end location had a marginal value of 50 mm and a marginal value of 52 mm at the inlet end. Under hot-shut down condition (calculated at hoop stress of 110 MPa and at 265 °C), the critical crack length would be only 43 mm [10].

Even though saturation vis-à-vis hydrogen pick-up has not been unambiguously established it is to be noted that the H_{eq} content of pressure tube J-07 (MAPS 1) was as high as 200 ppm at the inlet end and outlet end and about 70 ppm at mid-length. Such H_{eq} contents are neither likely to be expected nor advisable for continued pressure tube operation. Therefore the critical crack length derived from fracture toughness data for pressure tube J-07 (MAPS 1) can be used to estimate the end of life (EOL) of Zircaloy-2 pressure tubes in operating reactors.

The delayed hydride crack velocity of unirradiated Zircaloy-2 pressure tube at 300 °C is about 0.12 mm/h, as given in Table 4. It is expected that in irradiated pressure tubes, the value of DHC velocity would increase by a factor up to 5. This implies that a leaking crack in PT would require 20 h to grow to a critical size by DHC, if necessary conditions for DHC to occur are present. However, it may be noted that DHC crack did not grow in specimens having H_{eq} of 115 ppm even after six days when ΔT used was 30 °C (Table 4).

The model of creep and growth fitted to the measured diametral strain values is shown in Fig. 3. If the constants used in the constitutive equation are assumed to remain unchanged over the operating period, the total diametral increase corresponding to 30 EFPYs comes to be less than 3.0%. Thus, even for extended design life the diametral increase may remain below the allowed limit of 5%.

4.3. Garter springs

The stretch test results indicate that each link of the GS irrespective of the presence of solid hydride, if any, after 8.25 EFPY would withstand a minimum of 9 kg load, and a very high extent of stretching. This stretching was several times more than the space available between the two free ends of the GS to expand in the circular girdle wire. The tension test results indicate the distinct possibility of loading up to 20 kg. The details of stretch test and tension test are available elsewhere [4].

The crush test results indicate that the load needed to crush the coils (which would cause breakage of GS) should at least be of the order of 700 N/coil, which was more than one order in magnitude of the design load. Thus the results indicated that the GS after 8.25 EFPY of operation would have strength and ductility much greater than what is required in-service.

Inter comparison of the tension test results at corresponding EFPYs of 6.5 and 8.25, indicate the possibility of saturation in strength of GS at EFPYs higher than 6.5 [3]. Similar inter comparison of the crush test results rule out any dramatic reduction in the crushing load to a value that approaches the design crush load. Thus the GSs are likely to retain their integrity up to 8.25 EFPYs and possibly beyond.

4.4. Calandria tube

Irradiation induced growth under fast neutron irradiation is recognized as a major source of dimensional instability in calandria tubes in water cooled reactors. Experimental studies have established that irradiation growth in zirconium and its alloys is influenced by its metallurgical conditions (texture, grain size, dislocation density and alloy contents), manufacturing route (residual stress) and experimental conditions (irradiation temperatures and fast neutron fluence). Metallographic examination revealed that the seam welded specimen had grain size of 8–10 μm in the radial and circumferential direction and 22 μm in longitudinal direction. The weld region had a grain size of 78 μm in both radial and circumferential directions. Seamless CT specimens had a fine equiaxed grain structure, the grain size being 7–10 μm in radial-tangential plane and 21 μm in longitudinal direction. The seamless pilgered tube did not have a crystallographic texture substantially different from that of the welded tubes. No significant difference in the irradiation growth behaviour was found between these two types of tubes, as given in Table 5. The pilgered tubes, therefore, can be considered as good as the seam welded tubes so far as the texture is considered while they are distinctly superior, if grain size and absence of weld are considered.

5. Conclusion

A brief account of the work towards the assessment of ageing in different zirconium alloy components such as Zircaloy claddings, zirconium alloy pressure tubes, zirconium alloy garter springs and seamless Zircaloy calandria tubes has been presented. The methodologies adopted for conducting component specific tests are illustrated. Application of test results is elaborated for residual life estimation/life extension of these components.

References

[1] S. Chatterjee, S. Anantharaman, K.S. Balakrishnan, K.S. Sivaramakrishnan, ASTM STP 1046, ASTM (1990) 515–524.
[2] S. Chatterjee, H.K. Shriharsha, K.S. Balakrishnan, Report BARC/2001/E/027, Bhabha Atomic Research Centre, Mumbai, India, 2001.
[3] S. Chatterjee, S. Anantharaman, K.S. Balakrishnan, H.K. Shriharsha, Report BARC/1999/E/025, Bhabha Atomic Research Centre, Mumbai, India, 1999, pp. 1–21.
[4] S. Chatterjee, K.S. Balakrishnan, S. Anantharaman, Report BARC/1999/E/028, Bhabha Atomic Research Centre, Mumbai, India, 1999.

[5] N. Christodoulou, A.R. Causey, R.A. Holt, C.N. Tome, N. Badie, R.J. Klassen, R. Sauver, C.H. Woo, ASTM STP 1295 (1996) 518–537.
[6] P.K. Shah, H.K. Shriharsha, A.P. Kulkarni, K. Pandit, S. Chatterjee, M.P. Dhotre, S. Kumar, in: Proceedings of Symposium on Zirconium-2002, BARC, Mumbai, India, 11–13 September, 2002, pp. 487–491.
[7] G.F. Slattery, ASTM STP 458, ASTM (1970).
[8] K.S. Balakrishnan, S. Anantharaman, A.B. Tamhane, S. Chatterjee, in: Proceedings of Symposium on Zirconium-2002, BARC, Mumbai, India, 11–13 September, 2002, pp. 639–642.
[9] D.O. Pickman, Nucl. Eng. Des. 21 (1972) 212–236.
[10] S. Chatterjee, K.S. Balakrishnan, P.K. Shah, Report BARC/2004/E/007, Bhabha Atomic Research Centre, Mumbai, India, 2004.